Linearized buckling analysis of isotropic and composite beam-columns by Carrera Unified Formulation and Dynamic Stiffness Method

Linearized buckling analysis of isotropic and composite beam-columns by Carrera Unified Formulation and Dynamic Stiffness Method

E. Carrera[ab*], A. Pagani[ac†] and J. R. Banerjee[c‡]

[a]Department of Mechanical and Aerospace Engineering, Politecnico di Torino, Corso Duca degli Abruzzi 24, 10129 Torino, Italy.

[b]School of Aerospace, Mechanical and Manufacturing Engineering, RMIT University, Bundoora VIC 3083, Australia.

[c]School of Engineering and Mathematical Sciences, City University London, Northampton Square, London, EC1V 0HB, United Kingdom.

Submitted to:

Mechanics of Advanced Materials and Structures,

Special Issue dedicated to Carrera Unified Formulation

*Professor of Aerospace Structures and Aeroelasticity, e-mail: erasmo.carrera@polito.it
†**Author for correspondence**. Ph.D. Student, e-mail: alfonso.pagani@polito.it
‡Professor of Aeronautical Engineering, e-mail: J.R.Banerjee@city.ac.uk

Abstract

This paper introduces a one-dimensional (1D) higher-order exact formulation for linearized buckling analysis of beam-columns. The Carrera Unified Formulation (CUF) is utilised and the displacement field is expressed as a generic N-order expansion of the generalized unknown displacement field. The principle of virtual displacements is invoked along with CUF to derive the governing equations and the associated natural boundary conditions in terms of fundamental nuclei, which can be systematically expanded according to N by exploiting an extensive index notation. After the closed form solution of the N-order beam-column element is sought, an exact Dynamic Stiffness (DS) matrix is derived by relating the amplitudes of the loads to those of the responses. The global DS matrix is finally processed through the application of the Wittrick-Williams algorithm to extract the buckling loads of the structure. Isotropic solid and thin-walled cross-section beams as well as laminated composite structures are analysed in this paper. The validity of the formulation and its broad range of applicability are demonstrated through comparisons of results from the literature and by using commercial finite element codes.

Keywords: Carrera unified formulation; Dynamic stiffness method; Buckling; Higher-order theories; Thin-walled; Beams; Composites

1 Introduction

Buckling analysis of beam-columns has been widely investigated in the past and recent years because the subject matter plays an important role in the design of structures. Several methodologies have therefore been developed and there are excellent texts on the subject, see for example Timoshenko [1] and Matsunaga [2].

In most of the classical works on beam-column buckling, it has been assumed that when the equilibrium of the column is disturbed, it becomes unstable due to bending in the plane of smaller second moment of area. There are cases of practical interest where the column may buckle due to twisting or due to a combination of both twisting and bending. Such types of torsion or bending-torsion buckling are particularly relevant for thin-walled cross-sections. Some noteworthy contributions on instability of thin-walled columns are due to Wagner [3], Goodier [4] and Vlasov [5], amongst others. More recent papers on this topic can be found in Vo and Lee [6, 7] and Kim et al. [8]. In essence, Vo and Lee [6, 7] developed an analytical model based on the shear deformable beam theory whereas Kim et al. [8] proposed a formulation based on the displacement parameters defined at an arbitrarily chosen axis, including second-order terms of finite semi-tangential rotations. Furthermore, the applications of the generalized beam theory to stability analyses [9, 10] deserve some special mention. Other contributions on the subject include Zhang and Tong [11], Mohri et al. [12] and Beale et al. [13].

Buckling analysis of composite beam-columns, of course, merits a separate discussion. The classical theory based on Euler-Bernoulli beam model (EBBM) generally overestimates the critical buckling loads of short beams since it does not include transverse shear effects. By contrast, the Timoshenko beam model (TBM) accounts for the first-order shear deformation effects. However, TBM violates the zero shear stress condition on the un-loaded lateral surfaces of the beam. The correct implementation of shear phenomena is of fundamental importance for composite laminates because of their low transverse shear moduli compared to the axial tensile moduli, as discussed in the excellent review of Kapania and Raciti [14, 15] which also includes a comprehensive overview on composite beam works. Higher-order beam models for the stability analysis of composite beam-columns have been therefore given wide coverage in the literature. Some noteworthy contributions are those by Khedir and Reddy [16], Zhen and Wanji [17], Aydogdu [18], and Vo and Thai [19].

In the present work, a general formulation for buckling analysis of both solid and thin-walled isotropic as well as anisotropic beam-columns is proposed. The methodology can deal with pure bending or torsional buckling modes independently as well as allows for coupled bending-torsion instability phenomena and higher-order shear effects. In the formulation presented, both metallic and composite columns can be analysed with no restrictions on the cross-sectional geometry. This is achieved by making use of the Carrera Unified Formulation (CUF) [20], which has received wide attention in recent years [21, 22, 23, 24]. CUF enables the development of 1D displacement fields in an arbitrary, but kinematically enriched manner. The governing differential equations can, in fact, be written in terms of the fundamental nuclei that depend nether on the order of the theory nor on the cross-sectional geometry. In recent works, CUF has already been applied to

buckling analysis of columns by using both Finite Element Method (FEM) [25] and a Navier type solution [26]. As it is known, FEM is a widely used numerical method in solid mechanics which transforms the governing differential equations into a system of algebraic equations. However, only approximate solutions are given by FEM. On the other hand, if the Navier solution is used, no numerical approximations are made, but of course, only simply supported boundary conditions can be addressed.

A more powerful, but elegant approach for CUF theories can be achieved through the application of the Dynamic Stiffness Method (DSM), which was recently applied by Pagani et al. [27, 28, 29] for free vibration analysis of metallic and composite beams and plates. The DSM is appealing in free vibration and buckling analyses because unlike the FEM, it provides exact solution of the governing equations of a structure for any boundary conditions, once the initial assumptions on the displacements field have been made. The uncompromising accuracy of the DSM when dealing with buckling analysis has been demonstrated by Banerjee and Williams [30], Banerjee [31], Eisenberger and Reich [32], Eisenberger [33] and Abramovich et al. [34], amongst others.

In this paper, CUF is employed to formulate the governing equations of the N-order beam-column. DSM is subsequently used along with the algorithm of Wittrick and Williams [35] to compute the critical buckling loads of both isotropic and composite laminated beam-columns. The results are finally compared and contrasted with those from the literature and from commercial FEM codes.

2 Carrera Unified Formulation for Beams

2.1 Preliminaries

The adopted rectangular cartesian coordinate system is shown in Fig. 1, together with the geometry of a multi-layered structure. The cross-section of the beam lies on the xz-plane and it is denoted by Ω, whereas the boundaries over y are $0 \leq y \leq L$. Introducing the transposed displacement vector,

$$\mathbf{u}(x,y,z) = \left\{ \begin{array}{ccc} u_x & u_y & u_z \end{array} \right\}^T \tag{1}$$

The stress, $\boldsymbol{\sigma}$, and strain, $\boldsymbol{\epsilon}$, components are expressed in transposed forms as follows:

$$\boldsymbol{\sigma} = \left\{ \begin{array}{cccccc} \sigma_{yy} & \sigma_{xx} & \sigma_{zz} & \sigma_{xz} & \sigma_{yz} & \sigma_{xy} \end{array} \right\}^T, \quad \boldsymbol{\epsilon} = \left\{ \begin{array}{cccccc} \epsilon_{yy} & \epsilon_{xx} & \epsilon_{zz} & \epsilon_{xz} & \epsilon_{yz} & \epsilon_{xy} \end{array} \right\}^T \tag{2}$$

In the case of small displacements with respect to a characteristic dimension in the plane of Ω, the strain-displacement relations are

$$\boldsymbol{\epsilon} = \mathbf{D}\mathbf{u} \tag{3}$$

where $\mathbf{D}$ is the following linear differential operator matrix

$$\mathbf{D} = \begin{bmatrix} 0 & \frac{\partial}{\partial y} & 0 \\ \frac{\partial}{\partial x} & 0 & 0 \\ 0 & 0 & \frac{\partial}{\partial z} \\ \frac{\partial}{\partial z} & 0 & \frac{\partial}{\partial x} \\ 0 & \frac{\partial}{\partial z} & \frac{\partial}{\partial y} \\ \frac{\partial}{\partial y} & \frac{\partial}{\partial x} & 0 \end{bmatrix} \tag{4}$$

In this work, geometric non-linearities are introduced in the axial strain in the Green-Lagrange sense.

$$\epsilon_{yy}^{\mathrm{nl}} = \frac{1}{2}(u_{x,_y}^2 + u_{y,_y}^2 + u_{z,_y}^2) \tag{5}$$

The suffix after the comma in Eq. (5) denotes the derivatives with respect to that variable. Constitutive laws are now exploited to obtain stress components to give

$$\boldsymbol{\sigma} = \tilde{\mathbf{C}}\boldsymbol{\epsilon} \tag{6}$$

In the case of orthotropic material the matrix $\tilde{\mathbf{C}}$ is

$$\tilde{\mathbf{C}} = \begin{bmatrix} \tilde{C}_{33} & \tilde{C}_{23} & \tilde{C}_{13} & 0 & 0 & \tilde{C}_{36} \\ \tilde{C}_{23} & \tilde{C}_{22} & \tilde{C}_{12} & 0 & 0 & \tilde{C}_{26} \\ \tilde{C}_{13} & \tilde{C}_{12} & \tilde{C}_{11} & 0 & 0 & \tilde{C}_{16} \\ 0 & 0 & 0 & \tilde{C}_{44} & \tilde{C}_{45} & 0 \\ 0 & 0 & 0 & \tilde{C}_{45} & \tilde{C}_{55} & 0 \\ \tilde{C}_{36} & \tilde{C}_{26} & \tilde{C}_{16} & 0 & 0 & \tilde{C}_{66} \end{bmatrix} \tag{7}$$

Coefficients $\tilde{C}_{ij}$ depend on Young modulus and Poisson ratio as well as on the fiber orientation angle, θ, which is graphically defined in Fig. 2 where "1", "2", and "3" represent the cartesian axes of the material. For the sake of brevity, the expressions for the coefficients $\tilde{C}_{ij}$ are not reported here, but can be found in standard texts, see for example Tsai [36] and Reddy [37].

Within the framework of the CUF, the displacement field $\mathbf{u}(x, y, z)$ can be expressed as

$$\mathbf{u}(x, y, z) = F_\tau(x, z)\mathbf{u}_\tau(y), \qquad \tau = 1, 2, ..., M \tag{8}$$

where F_τ are the functions of the coordinates x and z on the cross-section. $\mathbf{u}_\tau$ is the vector of the *generalized* displacements, M stands for the number of the terms used in the expansion, and the repeated subscript,

τ, indicates summation. The choice of F_τ determines the class of the 1D CUF model that is required and subsequently to be adopted. According to Eq. (8), Taylor expansion (TE) 1D CUF models consist of a MacLaurin series that uses the 2D polynomials $x^i\ z^j$ as F_τ functions, where i and j are positive integers including zero. For instance, the displacement field of the second-order ($N = 2$) TE model can be expressed as

$$\begin{aligned} u_x &= u_{x_1} + x\ u_{x_2} + z\ u_{x_3} + x^2\ u_{x_4} + xz\ u_{x_5} + z^2\ u_{x_6} \\ u_y &= u_{y_1} + x\ u_{y_2} + z\ u_{y_3} + x^2\ u_{y_4} + xz\ u_{y_5} + z^2\ u_{y_6} \\ u_z &= u_{z_1} + x\ u_{z_2} + z\ u_{z_3} + x^2\ u_{z_4} + xz\ u_{z_5} + z^2\ u_{z_6} \end{aligned} \tag{9}$$

The order N of the expansion is set as an input option in the analysis; the integer N is arbitrary and it defines the order the beam theory. Classical EBBM and TBM can be realised by using a suitable F_τ expansions as explained in [20]. Classical theories and first-order models ($N = 1$) require the necessary assumption of reduced material stiffness coefficients to correct Poisson's locking (see [38]). In this paper, Poisson's locking is corrected according to the method outlined by Carrera et al. [20].

2.2 Governing differential equations of the N-order model

The principle of virtual displacements is used to derive the governing differential equations.

$$\delta L_{\text{int}} - \delta L_{\sigma^0_{\text{yy}}} = 0 \tag{10}$$

where L_{int} stands for the strain energy and $L_{\sigma^0_{\text{yy}}}$ is the work done by the axial pre-stress σ^0_{yy} on the corresponding non-linear strain $\epsilon^{\text{nl}}_{yy}$. δ stands for the usual virtual variation operator. The virtual variation of the strain energy is

$$\delta L_{\text{int}} = \int_V \delta\boldsymbol{\epsilon}^T \boldsymbol{\sigma}\, \mathrm{d}V \tag{11}$$

Equation (11) is rewritten using Eqs. (3), (6) and (8). After integrations by part, Eq. (11) reads

$$\delta L_{\text{int}} = \int_L \delta\mathbf{u}_\tau^T \mathbf{K}^{\tau s} \mathbf{u}_s\, \mathrm{d}y + \left[\delta\mathbf{u}_\tau^T \mathbf{\Pi}^{\tau s} \mathbf{u}_s\right]_{y=0}^{y=L} \tag{12}$$

where $\mathbf{K}^{\tau s}$ is the differential linear stiffness matrix and $\mathbf{\Pi}^{\tau s}$ is the matrix of the natural boundary conditions in the form of 3×3 fundamental nuclei. The components of $\mathbf{K}^{\tau s}$ are provided in the following and they are

referred to as $K^{\tau s}_{(ij)}$, where i is the row number ($i = 1, 2, 3$) and j denotes the column number ($j = 1, 2, 3$):

$$
\begin{aligned}
K^{\tau s}_{(11)} &= E^{22}_{\tau,_x s,_x} + E^{44}_{\tau,_z s,_z} + \left(E^{26}_{\tau,_x s} - E^{26}_{\tau s,_x}\right)\frac{\partial}{\partial y} - E^{66}_{\tau s}\frac{\partial^2}{\partial y^2} \\
K^{\tau s}_{(12)} &= E^{26}_{\tau,_x s,_x} + E^{45}_{\tau,_z s,_z} + \left(E^{23}_{\tau,_x s} - E^{66}_{\tau s,_x}\right)\frac{\partial}{\partial y} - E^{36}_{\tau s}\frac{\partial^2}{\partial y^2} \\
K^{\tau s}_{(13)} &= E^{12}_{\tau,_x s,_z} + E^{44}_{\tau,_z s,_x} + \left(E^{45}_{\tau,_z s} - E^{16}_{\tau s,_z}\right)\frac{\partial}{\partial y} \\
K^{\tau s}_{(21)} &= E^{26}_{\tau,_x s,_x} + E^{45}_{\tau,_z s,_z} + \left(E^{66}_{\tau,_x s} - E^{23}_{\tau s,_x}\right)\frac{\partial}{\partial y} - E^{36}_{\tau s}\frac{\partial^2}{\partial y^2} \\
K^{\tau s}_{(22)} &= E^{66}_{\tau,_x s,_x} + E^{55}_{\tau,_z s,_z} + \left(E^{36}_{\tau,_x s} - E^{36}_{\tau s,_x}\right)\frac{\partial}{\partial y} - E^{33}_{\tau s}\frac{\partial^2}{\partial y^2} \\
K^{\tau s}_{(23)} &= E^{16}_{\tau,_x s,_z} + E^{45}_{\tau,_z s,_x} + \left(E^{55}_{\tau,_z s} - E^{13}_{\tau s,_z}\right)\frac{\partial}{\partial y} \\
K^{\tau s}_{(31)} &= E^{44}_{\tau,_x s,_z} + E^{12}_{\tau,_z s,_x} + \left(E^{16}_{\tau,_z s} - E^{45}_{\tau s,_z}\right)\frac{\partial}{\partial y} \\
K^{\tau s}_{(32)} &= E^{45}_{\tau,_x s,_z} + E^{16}_{\tau,_z s,_x} + \left(E^{13}_{\tau,_z s} - E^{55}_{\tau s,_z}\right)\frac{\partial}{\partial y} \\
K^{\tau s}_{(33)} &= E^{44}_{\tau,_x s,_x} + E^{11}_{\tau,_z s,_z} + \left(E^{45}_{\tau,_x s} - E^{45}_{\tau s,_x}\right)\frac{\partial}{\partial y} - E^{55}_{\tau s}\frac{\partial^2}{\partial y^2}
\end{aligned}
\tag{13}
$$

The generic term $E^{\alpha\beta}_{\tau,_\theta s,_\zeta}$ above is a cross-sectional moment parameter

$$
E^{\alpha\beta}_{\tau,_\theta s,_\zeta} = \int_\Omega \tilde{C}_{\alpha\beta} F_{\tau,_\theta} F_{s,_\zeta}\, \mathrm{d}\Omega \tag{14}
$$

The suffix after the comma in Eq. (13) denotes the derivatives with respect to the corresponding variable. As far as the boundary conditions are concerned, the components of $\mathbf{\Pi}^{\tau s}$ are

$$
\begin{aligned}
&\Pi^{\tau s}_{(11)} = E^{26}_{\tau s,_x} + E^{66}_{\tau s}\frac{\partial}{\partial y}, \quad \Pi^{\tau s}_{(12)} = E^{66}_{\tau s,_x} + E^{36}_{\tau s}\frac{\partial}{\partial y}, \quad \Pi^{\tau s}_{(13)} = E^{16}_{\tau s} \\
&\Pi^{\tau s}_{(21)} = E^{23}_{\tau s,_x} + E^{36}_{\tau s}\frac{\partial}{\partial y}, \quad \Pi^{\tau s}_{(22)} = E^{36}_{\tau s,_x} + E^{33}_{\tau s}\frac{\partial}{\partial y}, \quad \Pi^{\tau s}_{(23)} = E^{13}_{\tau s,_z} \\
&\Pi^{\tau s}_{(31)} = E^{45}_{\tau s}, \qquad\qquad \Pi^{\tau s}_{(32)} = E^{55}_{\tau s,_z}, \qquad\qquad \Pi^{\tau s}_{(33)} = E^{45}_{\tau s,_x} + E^{55}_{\tau s}\frac{\partial}{\partial y}
\end{aligned}
\tag{15}
$$

The virtual variation of the axial pre-stress is

$$
\delta L_{\sigma^0_{\mathrm{yy}}} = \int_L \left(\int_\Omega \sigma^0_{yy} \delta\epsilon^{\mathrm{nl}}_{yy}\, \mathrm{d}\Omega \right) \mathrm{d}y \tag{16}
$$

After substituting Eqs. (8) and (5) into Eq. (16) and after performing integration by parts, one obtaines

$$
\delta L_{\sigma^0_{\mathrm{yy}}} = -\sigma^0_{yy} \int_L \delta\mathbf{u}^T_\tau \mathbf{K}^{\tau s}_{\sigma^0_{yy}} \mathbf{u}_s\, \mathrm{d}y + \sigma^0_{yy} \left[\delta\mathbf{u}^T_\tau \mathbf{\Pi}^{\tau s}_{\sigma^0_{yy}} \mathbf{u}_s \right]^{y=L}_{y=0} \tag{17}
$$

where $\mathbf{K}^{\tau s}_{\sigma^0_{yy}}$ is the fundamental nucleus of the differential geometric stiffness matrix.

$$
\mathbf{K}^{\tau s}_{\sigma^0_{yy}} = \begin{bmatrix} E_{\tau s}\frac{\partial^2}{\partial y^2} & 0 & 0 \\ 0 & E_{\tau s}\frac{\partial^2}{\partial y^2} & 0 \\ 0 & 0 & E_{\tau s}\frac{\partial^2}{\partial y^2} \end{bmatrix} \tag{18}
$$

where

$$E_{\tau s} = \int_{\Omega} F_{\tau} F_s \, \mathrm{d}\Omega \tag{19}$$

The components of $\mathbf{\Pi}^{\tau s}_{\sigma^0_{yy}}$ are

$$\mathbf{\Pi}^{\tau s}_{\sigma^0_{yy}} = \begin{bmatrix} E_{\tau s}\frac{\partial}{\partial y} & 0 & 0 \\ 0 & E_{\tau s}\frac{\partial}{\partial y} & 0 \\ 0 & 0 & E_{\tau s}\frac{\partial}{\partial y} \end{bmatrix} \tag{20}$$

Thus the explicit forms of the governing equations are

$$\begin{aligned}
\delta u_{x\tau}: \quad & (\sigma^0_{yy}E_{\tau s} - E^{66}_{\tau s})u_{xs,_{yy}} + \big(E^{26}_{\tau,_x s} - E^{26}_{\tau s,_x}\big)u_{xs,_y} + \big(E^{22}_{\tau,_x s,_x} + E^{44}_{\tau,_z s,_z}\big)u_{xs} \\
& - E^{36}_{\tau s}u_{ys,_{yy}} + \big(E^{23}_{\tau,_x s} - E^{66}_{\tau s,_x}\big)u_{ys,_y} + \big(E^{26}_{\tau,_x s,_x} + E^{45}_{\tau,_z s,_z}\big)u_{ys} \\
& + \big(E^{45}_{\tau,_z s} - E^{16}_{\tau s,_z}\big)u_{zs,_y} + \big(E^{44}_{\tau,_z s,_x} + E^{12}_{\tau,_x s,_z}\big)u_{zs} = 0 \\
\delta u_{y\tau}: \quad & - E^{36}_{\tau s}u_{xs,_{yy}} + \big(E^{66}_{\tau,_x s} - E^{23}_{\tau s,_x}\big)u_{xs,_y} + \big(E^{26}_{\tau,_x s,_x} + E^{45}_{\tau,_z s,_z}\big)u_{xs} \\
& + (\sigma^0_{yy}E_{\tau s} - E^{33}_{\tau s})u_{ys,_{yy}} + \big(E^{36}_{\tau,_x s} - E^{36}_{\tau s,_x}\big)u_{ys,_y} + \big(E^{66}_{\tau,_x s,_x} + E^{55}_{\tau,_z s,_z}\big)u_{ys} \\
& + \big(E^{55}_{\tau,_z s} - E^{13}_{\tau s,_z}\big)u_{zs,y} + \big(E^{16}_{\tau,_x s,_z} + E^{45}_{\tau,_z s,_x}\big)u_{zs} = 0 \\
\delta u_{z\tau}: \quad & \big(E^{16}_{\tau,_z s} - E^{45}_{\tau s,_z}\big)u_{xs,_y} + \big(E^{44}_{\tau,_x s,_z} + E^{12}_{\tau,_z s,_x}\big)u_{xs} \\
& + \big(E^{13}_{\tau,_z s} - E^{55}_{\tau s,_z}\big)u_{ys,_y} + \big(E^{45}_{\tau,_x s,_z} + E^{16}_{\tau,_z s,_x}\big)u_{ys} \\
& + (\sigma^0_{yy}E_{\tau s} - E^{55}_{\tau s})u_{zs,_{yy}} + \big(E^{45}_{\tau,_x s} - E^{45}_{\tau s,_x}\big)u_{zs,_y} + \big(E^{44}_{\tau,_x s,_x} + E^{11}_{\tau,_z s,_z}\big)u_{zs} = 0
\end{aligned} \tag{21}$$

Letting $\mathbf{P}_{\tau} = \left\{ \begin{array}{ccc} P_{x\tau} & P_{y\tau} & P_{z\tau} \end{array} \right\}^T$ to be the vector of the generalized forces, the natural boundary conditions are

$$\begin{aligned}
\delta u_{x\tau}: \quad & P_{xs} = (E^{66}_{\tau s} - \sigma^0_{yy}E_{\tau s})u_{xs,_y} + E^{26}_{\tau s,_x}u_{xs} + E^{36}_{\tau s}u_{ys,_y} + E^{66}_{\tau s,_x}u_{ys} + E^{16}_{\tau s,_z}u_{zs} \\
\delta u_{y\tau}: \quad & P_{ys} = E^{36}_{\tau s}u_{xs,_y} + E^{23}_{\tau s,_x}u_{xs} + (E^{33}_{\tau s} - \sigma^0_{yy}E_{\tau s})u_{ys,_y} + E^{36}_{\tau s,_x}u_{ys} + E^{13}_{\tau s,_z}u_{zs} \\
\delta u_{z\tau}: \quad & P_{zs} = E^{45}_{\tau s,_z}u_{xs} + E^{55}_{\tau s,_z}u_{ys} + (E^{55}_{\tau s} - \sigma^0_{yy}E_{\tau s})u_{zs,_y} + E^{45}_{\tau s,_x}u_{zs}
\end{aligned} \tag{22}$$

For a fixed approximation order N, Eqs. (21) and (22) have to be expanded using the indices τ and s in order to obtain the governing differential equations and the natural boundary conditions of the desired model.

Equation (21) is a set of three coupled ordinary differential equations and it can be written in a matrix form as follows:

$$\delta \mathbf{u}_\tau : \quad \mathbf{L}^{\tau s}\, \tilde{\mathbf{u}}_s = 0 \tag{23}$$

where

$$\tilde{\mathbf{u}}_s = \left\{ \begin{array}{ccccccccc} u_{xs} & u_{xs,_y} & u_{xs,_{yy}} & u_{ys} & u_{ys,_y} & u_{ys,_{yy}} & u_{zs} & u_{zs,_y} & u_{zs,_{yy}} \end{array} \right\}^T \tag{24}$$

and $\mathbf{L}^{\tau s}$ is the 3×9 fundamental nucleus which contains the coefficients of the ordinary differential equations. The components of matrix $\mathbf{L}^{\tau s}$ are provided below and they are referred to as $L^{\tau s}_{(ij)}$, where i is the row number $(i = 1, 2, 3)$ and j is the column number $(j = 1, 2, ..., 9)$

$$\begin{array}{lll} L^{\tau s}_{(11)} = E^{22}_{\tau,_x s,_x} + E^{44}_{\tau,_z s,_z}, & L^{\tau s}_{(12)} = E^{26}_{\tau,_x s} - E^{26}_{\tau s,_x}, & L^{\tau s}_{(13)} = \sigma^0_{yy} E_{\tau s} - E^{66}_{\tau s} \\ L^{\tau s}_{(14)} = E^{26}_{\tau,_x s,_x} + E^{45}_{\tau,_z s,_z}, & L^{\tau s}_{(15)} = E^{23}_{\tau s,_x} - E^{66}_{\tau s,_x}, & L^{\tau s}_{(16)} = -E^{36}_{\tau s} \\ L^{\tau s}_{(17)} = E^{12}_{\tau,_x s,_z} + E^{44}_{\tau,_z s,_x}, & L^{\tau s}_{(18)} = E^{45}_{\tau,_z s} - E^{16}_{\tau s,_z}, & L^{\tau s}_{(19)} = 0 \\ L^{\tau s}_{(21)} = E^{26}_{\tau,_x s,_x} + E^{45}_{\tau,_z s,_z}, & L^{\tau s}_{(22)} = E^{66}_{\tau,_x s} - E^{23}_{\tau s,_x}, & L^{\tau s}_{(23)} = -E^{36}_{\tau s} \\ L^{\tau s}_{(24)} = E^{66}_{\tau,_x s,_x} + E^{55}_{\tau,_z s,_z}, & L^{\tau s}_{(25)} = E^{36}_{\tau,_x s} - E^{36}_{\tau s,_x}, & L^{\tau s}_{(26)} = \sigma^0_{yy} E_{\tau s} - E^{33}_{\tau s} \\ L^{\tau s}_{(27)} = E^{16}_{\tau,_x s,_z} + E^{45}_{\tau,_z s,_x}, & L^{\tau s}_{(28)} = E^{55}_{\tau,_z s} - E^{13}_{\tau s,_z}, & L^{\tau s}_{(29)} = 0 \\ L^{\tau s}_{(31)} = E^{44}_{\tau,_x s,_z} + E^{12}_{\tau,_z s,_x}, & L^{\tau s}_{(32)} = E^{16}_{\tau,_z s,_x} - E^{45}_{\tau s,_z}, & L^{\tau s}_{(33)} = 0 \\ L^{\tau s}_{(34)} = E^{45}_{\tau,_x s,_z} + E^{16}_{\tau,_z s,_x}, & L^{\tau s}_{(35)} = E^{13}_{\tau,_z s} - E^{55}_{\tau s,_z}, & L^{\tau s}_{(36)} = 0 \\ L^{\tau s}_{(37)} = E^{44}_{\tau,_x s,_x} + E^{11}_{\tau,_z s,_z}, & L^{\tau s}_{(38)} = E^{45}_{\tau,_x s} - E^{45}_{\tau s,_x}, & L^{\tau s}_{(39)} = \sigma^0_{yy} E_{\tau s} - E^{55}_{\tau s} \end{array} \tag{25}$$

For a given expansion order, N, the equilibrium equations can be obtained in the form of Eq. (26) given below by expanding $\mathbf{L}^{\tau s}$ for $\tau = 1, 2, ..., (N+1)(N+2)/2$ and $s = 1, 2, ..., (N+1)(N+2)/2$ as shown in Fig. 3. It reads:

$$\mathbf{L}\, \tilde{\mathbf{u}} = 0 \tag{26}$$

In a similar way, the boundary conditions of Eqs. (22) can be written in a matrix form as

$$\delta \mathbf{u}_\tau : \quad \mathbf{P}_s = \mathbf{B}^{\tau s}\, \hat{\mathbf{u}}_s \tag{27}$$

where

$$\hat{\mathbf{u}}_s = \left\{ \begin{array}{cccccc} u_{xs} & u_{xs,_y} & u_{ys} & u_{ys,_y} & u_{zs} & u_{zs,_y} \end{array} \right\}^T \tag{28}$$

and $\mathbf{B}^{\tau s}$ is the 3×6 fundamental nucleus which contains the coefficients of the natural boundary conditions

$$\mathbf{B}^{\tau s} = \left[\begin{array}{cccccc} E^{26}_{\tau s,_x} & (E^{66}_{\tau s} - \sigma^0_{yy} E_{\tau s}) & E^{66}_{\tau s,_x} & E^{36}_{\tau s} & E^{16}_{\tau s,_z} & 0 \\ E^{23}_{\tau s,_x} & E^{36}_{\tau s} & E^{36}_{\tau s,_x} & (E^{33}_{\tau s} - \sigma^0_{yy} E_{\tau s}) & E^{13}_{\tau s,_z} & 0 \\ E^{45}_{\tau s,_z} & 0 & E^{55}_{\tau s,_z} & 0 & E^{45}_{\tau s,_x} & (E^{55}_{\tau s} - \sigma^0_{yy} E_{\tau s}) \end{array} \right] \tag{29}$$

For a given expansion order N, the natural boundary conditions can be obtained in the form of Eq. (30) by expanding $\mathbf{B}^{\tau s}$ in the same way as $\mathbf{L}^{\tau s}$ to finally give

$$\mathbf{P} = \mathbf{B}\, \hat{\mathbf{u}} \tag{30}$$

Matrices $\mathbf{L}$ and $\mathbf{B}$ are evaluated for each layer of the laminated beam; global matrices are then obtained by summing the contribution of each layer.

3 Solution of the Differential Equations

Equation (26) is a system of ordinary differential equations (ODEs) of second order in y with constant coefficients. A change of variables is used to reduce the second order system of ODEs to a first order system,

$$\begin{array}{l} \mathbf{Z} = \left\{ \begin{array}{cccc} Z_1 & Z_2 & \dots & Z_n \end{array} \right\}^T = \hat{\mathbf{u}} = \\ \left\{ \begin{array}{cccccccccccc} u_{x1} & u_{x1,_y} & u_{y1} & u_{y1,_y} & u_{z1} & u_{z1,_y} & \dots & u_{xM} & u_{xM,_y} & u_{yM} & u_{yM,_y} & u_{zM} & u_{zM,_y} \end{array} \right\}^T \end{array} \tag{31}$$

where $\hat{\mathbf{u}}$ is the expansion of $\hat{\mathbf{u}}_s$ for a given theory order, $M = (N+1)(N+2)/2$ is the number of expansion terms for the given N-order beam theory, and $n = 6 \times M$ is the dimension of the unknown vector as well as the number of differential equations. In [27], an automatic algorithm to transform the $\mathbf{L}$ matrix of Eq. (26) into the matrix $\mathbf{S}$ of the following linear differential system was described:

$$\mathbf{Z}'(y) = \mathbf{S}\mathbf{Z}(y) \tag{32}$$

Once the problem is described in terms of Eq. (32), the solution can be written as follows:

$$\begin{bmatrix} Z_1 \\ Z_2 \\ \vdots \\ Z_n \end{bmatrix} = \begin{bmatrix} \delta_{11} & \delta_{21} & \dots & \delta_{n1} \\ \delta_{12} & \delta_{22} & \dots & \delta_{n2} \\ \vdots & \vdots & \ddots & \vdots \\ \delta_{1n} & \delta_{2n} & \dots & \delta_{nn} \end{bmatrix} \begin{bmatrix} C_1 \mathrm{e}^{\lambda_1 y} \\ C_2 \mathrm{e}^{\lambda_2 y} \\ \vdots \\ C_n \mathrm{e}^{\lambda_n y} \end{bmatrix} \tag{33}$$

where λ_i is the i-th eigenvalue of the $\mathbf{S}$ matrix, δ_{ij} is the j-th element of the i-th eigenvector of the $\mathbf{S}$ matrix and C_i are the integration constants which need to be determined by using the boundary conditions. The above equation can be written in matrix form as:

$$\mathbf{Z} = \boldsymbol{\delta} \mathbf{C} \mathrm{e}^{\boldsymbol{\lambda} y} \tag{34}$$

It should be noted that the vector $\mathbf{Z}$ does not only contain the displacements but also their first derivatives which will come at hand when computing the boundary conditions. If only the displacements are needed, by recalling Eq. (31), only the rows $1, 3, 5, \dots, n-1$ should be taken into account, giving a solution in the following form:

$$\begin{aligned} u_{x1}(y) &= C_1 \delta_{11} \mathrm{e}^{\lambda_1 y} + C_2 \delta_{21} \mathrm{e}^{\lambda_2 y} + \dots + C_n \delta_{n1} \mathrm{e}^{\lambda_n y} \\ u_{y1}(y) &= C_1 \delta_{13} \mathrm{e}^{\lambda_1 y} + C_2 \delta_{23} \mathrm{e}^{\lambda_2 y} + \dots + C_n \delta_{n3} \mathrm{e}^{\lambda_n y} \\ u_{z1}(y) &= C_1 \delta_{15} \mathrm{e}^{\lambda_1 y} + C_2 \delta_{25} \mathrm{e}^{\lambda_2 y} + \dots + C_n \delta_{n5} \mathrm{e}^{\lambda_n y} \\ &\vdots \\ u_{zM}(y) &= C_1 \delta_{1(n-1)} \mathrm{e}^{\lambda_1 y} + C_2 \delta_{2(n-1)} \mathrm{e}^{\lambda_2 y} + \dots + C_n \delta_{n(n-1)} \mathrm{e}^{\lambda_n y} \end{aligned} \tag{35}$$

Once the displacements and their first derivatives are known, the boundary conditions can be easily obtained by remembering that $\hat{\mathbf{u}}$ is equal to $\mathbf{Z}$ (Eq. (31)) and by substituting the solution of Eq. (34) into the boundary conditions (Eq. (30)) to give

$$\mathbf{P} = \mathbf{B} \boldsymbol{\delta} \mathbf{C} \mathrm{e}^{\boldsymbol{\lambda} y} = \boldsymbol{\Lambda} \mathbf{C} e^{\boldsymbol{\lambda} y} \tag{36}$$

The boundary conditions can be written in explicit form as follows:

$$\begin{aligned} P_{x1}(y) &= C_1 \Lambda_{11} \mathrm{e}^{\lambda_1 y} + C_2 \Lambda_{12} \mathrm{e}^{\lambda_2 y} + \dots + C_n \Lambda_{1n} \mathrm{e}^{\lambda_n y} \\ P_{y1}(y) &= C_1 \Lambda_{21} \mathrm{e}^{\lambda_1 y} + C_2 \Lambda_{22} \mathrm{e}^{\lambda_2 y} + \dots + C_n \Lambda_{2n} \mathrm{e}^{\lambda_n y} \\ P_{z1}(y) &= C_1 \Lambda_{31} \mathrm{e}^{\lambda_1 y} + C_2 \Lambda_{32} \mathrm{e}^{\lambda_2 y} + \dots + C_n \Lambda_{3n} \mathrm{e}^{\lambda_n y} \\ &\vdots \\ P_{zM}(y) &= C_1 \Lambda_{n1} \mathrm{e}^{\lambda_1 y} + C_2 \Lambda_{n2} \mathrm{e}^{\lambda_2 y} + \dots + C_n \Lambda_{nn} \mathrm{e}^{\lambda_n y} \end{aligned} \tag{37}$$

The matrix $\mathbf{L}^{\tau s}$ is an efficient way to write the differential equations and the greatest advantage is that it allows for automatic formulation of the differential equations of any order beam theories in a systematic way. In sharp contrast to the structural problems solved in the literature, where by using a Navier-type solution or FEM the system becomes algebraic, here by using $\mathbf{L}$ the differential equations can be written automatically, thus allowing the exact solution for any-order theory possible with relative ease.

4 Dynamic Stiffness Method

4.1 Dynamic stiffness matrix

The procedure to obtain the DS matrix can be summarised as follows: (i) Seek a closed form analytical solution of the governing differential equations of the pre-stressed structural element; (ii) Apply a number of general boundary conditions equal to twice the number of integration constants in algebraic form which are usually the nodal displacements and forces; (iii) Eliminate the integration constants by relating the generalized nodal forces to the corresponding generalized displacements which generates the DS matrix. The closed form solution has already been found in the previous section and now the generic boundary conditions for generalized displacements and forces need to be applied (see Fig. 4) to develop the DS matrix.

Starting from the displacements, the boundary conditions can be written as

$$\begin{aligned}
&\text{At} \quad y = 0 \ : \\
&\qquad u_{x1}(0) = -\overline{U}1_{x1} \\
&\qquad u_{y1}(0) = -\overline{U}1_{y1} \\
&\qquad u_{z1}(0) = -\overline{U}1_{z1} \\
&\qquad \vdots \\
&\qquad u_{zM}(0) = -\overline{U}1_{zM}
\end{aligned} \tag{38}$$

$$\begin{aligned}
&\text{At} \quad y = L \ : \\
&\qquad u_{x1}(L) = \overline{U}2_{x1} \\
&\qquad u_{y1}(L) = \overline{U}2_{y1} \\
&\qquad u_{z1}(L) = \overline{U}2_{z1} \\
&\qquad \vdots \\
&\qquad u_{zM}(L) = \overline{U}2_{zM}
\end{aligned} \tag{39}$$

By evaluating Eqs. (35) in 0 and L and applying the boundary conditions of Eq.s (38) and (39), the following

matrix relation for the nodal displacements is obtained:

$$\begin{Bmatrix} \overline{U}1_{x1} \\ \overline{U}1_{y1} \\ \overline{U}1_{z1} \\ \vdots \\ \overline{U}1_{zM} \\ \overline{U}2_{x1} \\ \overline{U}2_{y1} \\ \overline{U}2_{z1} \\ \vdots \\ \overline{U}2_{zM} \end{Bmatrix} = \begin{bmatrix} -\delta_{11} & -\delta_{21} & \dots & -\delta_{n1} \\ -\delta_{13} & -\delta_{23} & \dots & -\delta_{n3} \\ -\delta_{15} & -\delta_{25} & \dots & -\delta_{n5} \\ \vdots & \vdots & \ddots & \vdots \\ -\delta_{1(n-1)} & -\delta_{2(n-1)} & \dots & -\delta_{n(n-1)} \\ \delta_{11}\mathrm{e}^{\lambda_1 L} & \delta_{21}\mathrm{e}^{\lambda_2 L} & \dots & \delta_{n1}\mathrm{e}^{\lambda_n L} \\ \delta_{13}\mathrm{e}^{\lambda_1 L} & \delta_{23}\mathrm{e}^{\lambda_2 L} & \dots & \delta_{n3}\mathrm{e}^{\lambda_n L} \\ \delta_{15}\mathrm{e}^{\lambda_1 L} & \delta_{25}\mathrm{e}^{\lambda_2 L} & \dots & \delta_{n5\mathrm{e}^{\lambda_n L}} \\ \vdots & \vdots & \ddots & \vdots \\ \delta_{1(n-1)}\mathrm{e}^{\lambda_1 L} & \delta_{2(n-1)}\mathrm{e}^{\lambda_2 L} & \dots & \delta_{n(n-1)}\mathrm{e}^{\lambda_n L} \end{bmatrix} \begin{Bmatrix} C_1 \\ C_2 \\ C_3 \\ \vdots \\ C_{\frac{n}{2}} \\ C_{\frac{n}{2}+1} \\ C_{\frac{n}{2}+2} \\ C_{\frac{n}{2}+3} \\ \vdots \\ C_n \end{Bmatrix} \tag{40}$$

The above equation can be written in a more compact form as

$$\overline{\mathbf{U}} = \mathbf{AC} \tag{41}$$

Similarly, boundary conditions for generalized nodal forces are as follows:

$$\begin{aligned} &\text{At} \quad y = 0 : \\ &\qquad P_{x1}(0) = -\overline{P}1_{x1} \\ &\qquad P_{y1}(0) = -\overline{P}1_{y1} \\ &\qquad P_{z1}(0) = -\overline{P}1_{z1} \\ &\qquad \vdots \\ &\qquad P_{zM}(0) = -\overline{P}1_{zM} \end{aligned} \tag{42}$$

$$\begin{aligned} &\text{At} \quad y = L : \\ &\qquad P_{x1}(L) = \overline{P}2_{x1} \\ &\qquad P_{y1}(L) = \overline{P}2_{y1} \\ &\qquad P_{z1}(L) = \overline{P}2_{z1} \\ &\qquad \vdots \\ &\qquad P_{zM}(L) = \overline{P}2_{zM} \end{aligned} \tag{43}$$

By evaluating Eqs. (37) in 0 and L and applying the BCs of Eq.s (42) and (43), the following matrix relation

for the nodal forces is obtained:

$$\begin{Bmatrix} \overline{P}1_{x1} \\ \overline{P}1_{y1} \\ \overline{P}1_{z1} \\ \vdots \\ \overline{P}1_{M1} \\ \overline{P}2_{x1} \\ \overline{P}2_{y1} \\ \overline{P}2_{z1} \\ \vdots \\ \overline{P}2_{M1} \end{Bmatrix} = \begin{bmatrix} -\Lambda_{11} & -\Lambda_{12} & \dots & -\Lambda_{1n} \\ -\Lambda_{21} & -\Lambda_{22} & \dots & -\Lambda_{2n} \\ -\Lambda_{31} & -\Lambda_{32} & \dots & -\Lambda_{3n} \\ \vdots & \vdots & \ddots & \vdots \\ -\Lambda_{n1} & -\Lambda_{n2} & \dots & -\Lambda_{nn} \\ \Lambda_{11}\mathrm{e}^{\lambda_1 L} & \Lambda_{12}\mathrm{e}^{\lambda_2 L} & \dots & \Lambda_{1n}\mathrm{e}^{\lambda_n L} \\ \Lambda_{21}\mathrm{e}^{\lambda_1 L} & \Lambda_{22}\mathrm{e}^{\lambda_2 L} & \dots & \Lambda_{2n}\mathrm{e}^{\lambda_n L} \\ \Lambda_{31}\mathrm{e}^{\lambda_1 L} & \Lambda_{32}\mathrm{e}^{\lambda_2 L} & \dots & \Lambda_{3n}\mathrm{e}^{\lambda_n L} \\ \vdots & \vdots & \ddots & \vdots \\ \Lambda_{n1}\mathrm{e}^{\lambda_1 L} & \Lambda_{n2}\mathrm{e}^{\lambda_2 L} & \dots & \Lambda_{nn}\mathrm{e}^{\lambda_n L} \end{bmatrix} \begin{Bmatrix} C_1 \\ C_2 \\ C_3 \\ \vdots \\ C_{\frac{n}{2}} \\ C_{\frac{n}{2}+1} \\ C_{\frac{n}{2}+2} \\ C_{\frac{n}{2}+3} \\ \vdots \\ C_n \end{Bmatrix} \tag{44}$$

The above equation can be written in a more compact form as

$$\overline{\mathbf{P}} = \mathbf{R}\mathbf{C} \tag{45}$$

The constants vector $\mathbf{C}$ from Eqs. (41) and (45) can now be eliminated to give the DS matrix of one beam element as follows:

$$\overline{\mathbf{P}} = \boldsymbol{\mathcal{K}}\overline{\mathbf{U}} \tag{46}$$

where

$$\boldsymbol{\mathcal{K}} = \mathbf{R}\mathbf{A}^{-1} \tag{47}$$

is the required DS matrix, which is the basic building block to compute the exact buckling loads of a higher-order beam-columns. The DSM has also many of the general features of the FEM. In particular, it is possible to assemble elemental DS matrices to form the overall DS matrix of any complex structures consisting of beam elements (see Fig. 5). The global DS matrix can be written as

$$\overline{\mathbf{P}}_{\mathrm{G}} = \boldsymbol{\mathcal{K}}_{\mathrm{G}}\overline{\mathbf{U}}_{\mathrm{G}} \tag{48}$$

where $\boldsymbol{\mathcal{K}}_G$ is the square global DS matrix of the final structure. For the sake of simplicity, the subscript "G" is omitted hereinafter.

As far as the boundary conditions are concerned, they can be applied by using either the well-known penalty method (often used in FEM) or by simply removing rows and columns of the stiffness matrix corresponding to the degrees of freedom which need to be suppressed.

4.2 Eigenvalues and eigenmodes calculation

For linearized buckling analysis of structures, FEM generally leads to a linear eigenvalue problem. By contrast, the DSM leads to a transcendental (non-linear) eigenvalue problem for which the Wittrick-Williams algorithm

[39] is recognisably the best available solution technique at present. The basic working principle of the algorithm can be briefly summarised in the following steps:

(i) A trial critical load $-\sigma_{yy}^{0} = \lambda^{*}$ is chosen to compute the dynamic stiffness matrix $\boldsymbol{\mathcal{K}}^{*}$ of the final structure;

(ii) $\boldsymbol{\mathcal{K}}^{*}$ is reduced to its upper triangular form by the usual form of Gauss elimination to obtain $\boldsymbol{\mathcal{K}}^{*^{\triangle}}$ and the number of negative terms on the leading diagonal of $\boldsymbol{\mathcal{K}}^{*^{\triangle}}$ is counted; this is known as the sign count $s(\boldsymbol{\mathcal{K}}^{*})$ of the algorithm;

(iii) The number, j, of critical loads (λ) of the structure which lie below a trial buckling load (λ^{*}) is given by:

$$j = j_0 + s(\boldsymbol{\mathcal{K}}^{*}) \tag{49}$$

where j_0 is is the number of critical buckling loads of all individual elements with clamped-clamped (CC) boundary conditions on their opposite sides which still lie below the trial critical buckling load λ^{*}.

Note that j_0 is required because the DSM allows for an infinite number of critical buckling loads to be accounted for when all the nodes of the structure are fully clamped so that one or more individual elements of the structure can still buckle on their own between the nodes. j_0 corresponds to $\overline{\mathbf{U}} = 0$ modes of Eq. (48) when $\overline{\mathbf{P}} = 0$. Assuming that j_0 is known, and $s(\boldsymbol{\mathcal{K}}^{*})$ can be obtained by counting the number of negative terms in $\boldsymbol{\mathcal{K}}^{*^{\triangle}}$, a suitable procedure can be devised, for example the bi-section method, to bracket any critical load between an upper and lower bound of the trial load λ^{*} to any desired accuracy. The computation of j_0 can be cumbersome and may require additional analysis to compute the clamped-clamped (CC) buckling loads of the single elements within the structure. The problem can be overcome by splitting the element into many smaller elements for which the CC critical loads will be exceptionally high and hence j_0 will be zero within all practical range of interest.

Once the critical buckling loads have been computed and the related global DS matrix evaluated, the corresponding nodal generalized displacements can be obtained by solving the associated homogeneous system of Eq. (48). By utilizing the nodal generalized displacements $\overline{\mathbf{U}}$, the integration constants $\mathbf{C}$ of the element can be computed with the help of Eq. (41). In this way, using Eq. (35), the unknown generalized displacements can be computed as a function of y. Finally, by using Eq. (8), the complete displacement field can be generated as a function of x, y, z. Clearly, the plot of the required mode shapes can be visualised on a fictitious 3D mesh. By following this procedure it is possible to compute the exact buckling modes using just one element which is, of course, impossible in FEM.

5 Numerical Results

In this section, the present 1D higher-order DS elements are used to compute the numerical results. First, a compact metallic beam is considered. Then, thin-walled structures are analysed to show the capability of the present CUF-DSM formulation to deal with coupled torsional-bending buckling phenomena. Symmetric and anti-symmetric cross-ply laminated composite beams are finally addressed. The results are compared with those from the literature and in some cases with those from 3D FEM models by using commercial codes.

5.1 Metallic rectangular cross-section beam

A cantilever metallic beam is analysed as the first illustrative example. The same structure was addressed in [2, 25], whose results are quoted hereafter for comparison purposes. The beam has a solid rectangular cross-section as shown in Fig. 6 and the material is aluminium alloy with elastic modulus $E = 71.7$ GPa and Poisson's ratio $\nu = 0.3$.

Table 1 shows the first three critical buckling loads for a length-to-height ratio, L/h, equal to 20. Critical loads are given in non-dimensional form as follows:

$$P^*_{cr} = \frac{P_{cr} L^2}{\pi^2 EI} \tag{50}$$

where I is the moment of inertia, $I = \frac{bh^3}{12}$. The second column of Table 1 shows the n-th non-dimensional critical buckling load from the Euler buckling formula give by

$$P^*_{cr_{Euler}} = n^2 \tag{51}$$

In column 3 the results by Matsunaga [2] are given whereas columns 4 to 7 report the results by classical and refined models based on TE CUF models of the present paper. The exact solution by the present DSM are compared to those from FEM, which was used in [25].

Figure 7 shows the variation of the first non-dimensional critical buckling load versus the length-to-side ratio, L/h, for different higher-order beam models by the present approach and the results are compared to those from [2] and from classical Euler ones. The same results are given in tabular form in Table 2.

The following comments arise from the analysis:

- Refined theories are mandatory when dealing with buckling analysis of short beam-columns.
- Euler buckling formula overestimates the critical loads of the beam-columns, even sometimes when a high length-to-side ratio is considered.
- Higher-order CUF theories are effective in refining the solution and the results are in good agreement with those available in the literature.

- The critical buckling load becomes lower as the expansion order for TE CUF models increases. This is significant because other theories give unconservative estimates of critical buckling loads, which can be dangerous.

- The exact solutions provided with the DSM is slightly higher then those by FEM. This is unusual and may be due to numerical problems inherent in FEM.

5.2 Thin-walled symmetric and non-symmetric cross-sections

The cantilever C-shaped section beam of Fig. 8 is now addressed. The main dimensions of the cross-section are $a_1 = 4$ cm, $a_2 = 2$ cm, $h = 10$ cm and $t = 0.5$ cm. The beam has a length $L = 2$ m and is made of homogeneous isotropic material with elastic modulus $E = 3 \times 10^4$ N/cm^2 and shear modulus $G = 1.15 \times 10^4$ N/cm^2.

Table 3 shows the first three critical buckling loads by higher-order beam models by the present CUF-DSM methodology. The results are compared with those given by Vo and Lee [6], who developed an analytical model based on the shear deformable beam theory, and those from [8], where a general formulation for spatial free vibration and stability analysis of non-symmetric thin-walled DS space frame members considering the effects of shear deformations was presented. A FEM solution from ABAQUS is also provided by [8]. Figure 9 shows the second buckling mode by the seventh-order ($N = 7$) CUF-DSM model. The figure clearly shows that the present method can predict the flexural-torsional buckling load accurately. The analysis highlights that

- Relatively higher-order kinematics are needed to detect flexural-torsional buckling modes of axially loaded thin-walled structures accurately.

- The results by the proposed CUF-DSM models are in good agreement with the results found in the literature.

A hollow square cross-section beam is further considered. The cross-section, which is shown in Fig. 10, has each side equal to $a = 0.1$ m and the uniform thickness equal to $t = a/20$. The whole structure is made of the same aluminium alloy as in the case of the rectangular solid cross-section beam-column. The critical buckling loads for various length-to-side ratios, L/a, are shown in Table 4, where the results by the present CUF-DSM methodology are compared to those from Giunta and al. [40], who adopted Navier-type solutions for simply-supported (SS) CUF beams and 3D FE models by ANSYS. It is clear that DSM can provide analytical solutions for CUF models, which exhibit 3D capabilities as the expansion order N is increased. Table 5 shows the first four buckling modes for the slender configuration, $L/a = 100$. The i-th mode is characterized by having i half-waves in the axial direction of the beam. It is clear from the analysis that, in the case of the slender beams, classical theories yield acceptable results unless higher buckling modes are considered. In the case of short beams (e.g. $L/a = 15$), refined beam models are necessary to obtain a 3D-like solution.

5.3 Cross-ply laminae

In this section a number of cross-ply laminated beam-columns are addressed and their stability characteristics are investigated. First, simply supported (SS) composite beam-columns with symmetric cross-ply [0°/90°/0°] and anti-symmetric cross-ply [0°/90°] stacking sequences are considered. Each lamina has the same thickness and two different sets of material properties are considered as follows:

$$\text{Material set I:} \quad E_1/E_2 = 10,\ G_{12} = G_{13} = 0.6E_2,\ G_{23} = 0.5E_2,\ \nu_{12} = 0.25$$

$$\text{Material set II:} \quad E_1/E_2 = 10,\ G_{12} = G_{13} = 0.5E_2,\ G_{23} = 0.2E_2,\ \nu_{12} = 0.25$$

The critical buckling loads from the present higher-order CUF-DSM refined beam theories are shown in Table 6 and they are given in the following non-dimensional form:

$$P^*_{cr} = \frac{P_{cr}L^2}{E_2bh^3} \tag{52}$$

In Table 6 the proposed solutions are compared to those available in the literature, see Vo and Thai [19] and Aydogdu [18]. The former [19] used FEM in conjunction with both a first-order beam theory (FOBT) and a higher-order beam theory (HOBT) accounting for the parabolic variation od shear strains through the thickness. The latter [18] proposed a three-degree-of-freedom shear deformable beam theory and the Ritz method was used to carry out stability analyses. The following comments are noteworthy:

- The present formulation can deal with the linearized stability analysis of composite laminated beam-columns.
- The solutions from both first- and higher-order beam models from the literature can be improved by the present CUF-DSM theories, especially when short beams and softer materials (e.g. Material set II) are considered.

In the last illustrative example, a rectangular beam with symmetric cross-ply $[0°/90°/0°/90°]_s$ arrangements is considered. The laminate is made of eight identical graphite/epoxy plies. The material has the following characteristics: $E_1 = 1.344 \times 10^5$ MPa, $E_2 = E_3 = 1.034 \times 10^4$ MPa, $G_{12} = G_{13} = 4.999 \times 10^3$ MPa, $G_{23} = 1.999 \times 10^3$ MPa, $\nu_{12} = \nu_{13} = \nu_{23} = 0.33$. The beam-column has length $L = 127$ mm, width $b = 12.7$ mm, and height $h = 10.16$ mm. Table 7 shows the critical buckling loads of this beam-column for both clamped-free (CF) and clamped-clamped (C-C) boundary conditions. Classical EBBM and up to the fifth-order ($N = 5$) CUF-DSM beam models are used for the results given in Table 7, which are compared to those provided by Chattopadhyay and Radu [41], who used the classical lamination plate theory (CLPT), the first-order shear deformation theory (FSDT), and a higher-order plate theory (HOT) to carry out instability analyses of composite plates. The analysis clearly demonstrates the capability of the present beam-column modelling technique, which is able to reproduce and to some extent refine the solutions from 2D plate models.

6 Conclusions

Higher-order theories and exact solutions for buckling analysis of beam-columns have been presented in this paper. Carrera Unified Formulation (CUF) has been employed along with the principle of virtual displacements to formulate the governing differential equations and the natural boundary conditions of beam-columns in terms of fundamental nuclei. These nuclei do not depend on the theory-order N, which is a free parameter of the formulation. The Dynamic Stiffness Method (DSM) has then been used in conjunction with the Wittrick-Williams algorithm to carry out stability analyses for both isotropic and anisotropic beam-columns. Both solid and thin-walled cross-sections have been analysed and the results have been compared with those available in the literature. The analysis demonstrates the need for higher-order models when dealing with short beams, shear deformable materials (e.g. composites), and thin-walled cross-sections. The validity of the present methodology is fully established. Further research could be aimed at extending the present CUF-DSM formulation for vibration analysis of axially loaded higher-order beams.

References

[1] S. P. Timoshenko. *Theory of elastic stability*. McGraw-Hill, 1961.

[2] H. Matsunaga. Buckling instabilities of thick elastic beams subjected to axial stress. *Computers & Structures*, 59(5):859–868, 1996.

[3] H. Wagner. Torsion and buckling of open sections. *Technical Memorandum No. 807, National Advisory Committee for Aeronautics*, 1936.

[4] J.N. Goodier. Flexural-torsional buckling of bars of open section under bending, eccentric thrust or torsional loads. *Cornell University Engineering Experimental Station Bulletin*, 28, 1942.

[5] V. Z. Vlasov. *Thin-walled elastic beams*. National Science Foundation, Washington, 1961.

[6] T.P. Vo and J. Lee. Flexuraltorsional coupled vibration and buckling of thin-walled open section composite beams using shear-deformable beam theory. *International Journal of Mechanical Sciences*, 51:631–641, 2009.

[7] T.P. Vo and H.-T. Thai. Vibration and buckling of composite beams using refined shear deformation theory. *International Journal of Mechanical Sciences*, 62:67–76, 2012.

[8] M.-Y. Kim, N.II Kim, and H.-T. Yun. Exact dynamic and static stiffness matrices of shear deformable thin-walled beam-columns. *Journal of Sound and Vibration*, 267:29–55, 2003.

[9] R. Schardt. Generalized beam theory an adequate method for coupled stability problems. *Thin-Walled Structures*, 19:161–180, 1994.

[10] P.B. Dinis, D. Camotim, and N. Silvestre. GBT formulation to analyse the buckling behaviour of thin-walled members with arbitrarily 'branched' open cross-sections. *Thin-Walled Structures*, 44(1):20–38, 2006.

[11] L. Zhang and G. Tong. Flexural-torsional buckling of thin-walled beam members based on shell buckling theory. *Thin-Walled Structures*, 42(12):1665–1687, 2004.

[12] F. Mohri, L. Azrar, and M. Potier-Ferryc. Flexural-torsional post-bickling analysis of thin-walled elements with open section. *Thin-Walled Structures*, 39(11):907–938, 2001.

[13] R.G. Beale, M.H.R. Godley, and V. Enjily. A theoretical and experimental investigation into cold-formed channel sections in bending with the unstiffened flanges in compression. *Computers and Structures*, 79(26–28):2403–2411, 2001.

[14] K. Kapania and S. Raciti. Recent advances in analysis of laminated beams and plates, part I: Shear effects and buckling. *AIAA Journal*, 27(7):923–935, 1989.

[15] K. Kapania and S. Raciti. Recent advances in analysis of laminated beams and plates, part II: Vibrations and wave propagation. *AIAA Journal*, 27(7):935–946, 1989.

[16] A.A. Khdeir and J.N. Reddy. Buckling of cross-ply laminated beams with arbitrary boundary conditions. *Composite Structures*, 37(1):1–3, 1997.

[17] W. Zhen and C. Wanji. An assessment of several displacement-based theories for the vibration and stability analysis of laminated composite and sandwich beams. *Composite Structures*, 84(4):337–349, 2008.

[18] M. Aydogdu. Buckling analysis of cross-ply laminated beams with general boundary conditions by Ritz method. *Composites Science and Technology*, 66(10):1248–1255, 2006.

[19] T.P. Vo and H.-T. Thai. Vibration and buckling of composite beams using refined shear deformation theory. *International Journal of Mechanical Sciences*, 62:67–76, 2012.

[20] E. Carrera, G. Giunta, and M. Petrolo. *Beam Structures: Classical and Advanced Theories*. John Wiley & Sons, 2011.

[21] M. Petrolo, E. Zappino, and E. Carrera. Refined free vibration analysis of one-dimensional structures with compact and bridge-like cross-sections. *Thin-Walled Structures*, 56:49–61, 2012.

[22] E. Carrera, A. Pagani, and F. Zangallo. Thin-walled beams subjected to load factors and non-structural masses. *International Journal of Mechanical Sciences*, 81:109–119, 2014.

[23] E. Carrera, A. Pagani, and M. Petrolo. Classical, refined and component-wise theories for static analysis of reinforced-shell wing structures. *AIAA Journal*, 51(5):1255–1268, 2013.

[24] E. Carrera and A. Pagani. Multi-line enhanced beam model for the analysis of laminated composite structures. *Composites Part B: Engineering*, 57(0):112–119, 2014.

[25] S.M. Ibrahim, E. Carrera, M. Petrolo, and E. Zappino. Buckling of composite thin walled beams by refined theory. *Composite Structures*, 94:563–570, 2012.

[26] G. Giunta, S. Belouettar, F. Biscani, and E. Carrera. Hierarchical theories for a linearised stability analysis of thin-walled beams with open and closed cross-section. *Advances in Aircraft and Spacecraft Science*, 1(3), 2014.

[27] A. Pagani, M. Boscolo, J.R. Banerjee, and E. Carrera. Exact dynamic stiffness elements based on one-dimensional higher-order theories for free vibration analysis of solid and thin-walled structures. *Journal of Sound and Vibration*, 332(23):6104–6127, 2013.

[28] A. Pagani, E. Carrera, M. Boscolo, and J.R. Banerjee. Refined dynamic stiffness elements applied to free vibration analysis of generally laminated composite beams with arbitrary boundary conditions. *Composite Structures*, 110(23):305–316, 2014.

[29] A. Pagani, E. Carrera, J.R. Banerjee, P.H. Cabral, G. Caprio, and A. Prado. Free vibration analysis of composite plates by higher-order 1D dynamic stiffness elements and experiments. *Composite Structures*, 118:654–663, 2014.

[30] J. R. Banerjee and F.W. Williams. The effect of shear deformation on the critical buckling of columns. *Journal of Sound and Vibration*, 174(5):607–616, 1994.

[31] J. R. Banerjee. Dynamic stiffness formulation for structural elements: a general approach. *Computers and Structures*, 63(1):101–103, 1997.

[32] M. Eisenberger and Y. Reich. Static, vibration and stability analysis of non-uniform beams. *Computers & Structures*, 31(4):567–573, 1989.

[33] M. Eisenberger. Buckling loads for variable cross-section members with variable axial forces. *International Journal of Solids and Structures*, 27(2):135–143, 1991.

[34] H. Abramovich, M. Eisenberger, and O. Shulepov. Vibrations and buckling of cross-ply nonsymmetric laminated composite beams. *AIAA Journal*, 34(5):1064–1069, 1996.

[35] W. H. Wittrick and F. W. Williams. A general algorithm for computing natural frequencies of elastic structures. *Quarterly Journal of Mechanics and Applied Mathematics*, 24(3):263–284, 1971.

[36] S. W. Tsai. *Composites Design*. Dayton, Think Composites, 4th edition, 1988.

[37] J. N. Reddy. *Mechanics of laminated composite plates and shells. Theory and Analysis*. CRC Press, 2nd edition, 2004.

[38] E. Carrera and S. Brischetto. Analysis of thickness locking in classical, refined and mixed multilayered plate theories. *Composite Structures*, 82(4):549–562, 2008.

[39] W. H. Wittrick and F. W. Williams. A general algorithm for computing natural frequencies of elastic structures. *Quarterly Journal of mechanics and applied sciences*, 24(3):263–284, 1970.

[40] G. Giunta, S. Belouettar, F. Biscani, and E. Carrera. Hierarchical theories for a linearized stability analysis of thin-walled beams with open and closed cross-section. *Advances in Aircraft and Spacecraft Science*, 1(3):253–271, 2014.

[41] A. Chattopadhyay and A.G. Radu. Dynamic instability of composite laminates using a higher order theory. *Computers and Structures*, 77:453–460, 2000.

Tables

Mode	Euler	Matsunaga [2]	TBM		N=1		N=2		N=3	
			FEM [25]	DSM	FEM [25]	DSM	FEM [25]	DSM	FEM [25]	DSM
1	1.000	0.992	0.990	0.993	0.993	0.993	0.993	0.993	0.992	0.992
2	4.000	3.873	3.875	3.886	3.884	3.886	3.885	3.887	3.873	3.874
3	9.000	8.387	8.422	8.444	8.437	8.444	8.444	8.451	8.387	8.391

Table 1: First three non-dimensional buckling loads ($P^*_{cr} = \frac{P_{cr}L^2}{\pi^2 EI}$) of the metallic beam, $L/h = 20$.

L/h	Euler	Matsunaga [2]	Present CUF-DSM			
			N=2	N=3	N=4	N=5
2	1.000	0.5723	0.5999	0.5741	0.5733	0.5730
4	1.000	0.8342	0.8497	0.8350	0.8349	0.8348
5	1.000	0.8860	0.8973	0.8866	0.8866	0.8865
10	1.000	0.9683	0.9718	0.9685	0.9685	0.9685
20	1.000	0.9919	0.9930	0.9919	0.9919	0.9919

Table 2: First non-dimensional buckling load ($P^*_{cr} = \frac{P_{cr}L^2}{\pi^2 EI}$) of the metallic beam for different length-to-height ratios L/h.

Mode	Present CUF-DSM							ABAQUS [8]	Kim et al. [8]	Vo and Lee [6]
	$N = 2$	$N = 3$	$N = 4$	$N = 5$	$N = 6$	$N = 7$	$N = 8$			
1	14.227	14.227	14.178	14.178	14.111	14.111	13.875	14.001	13.789	12.977
2	127.805	127.242	125.076	122.885	120.428	119.034	117.375	113.100	111.840	113.440
3	212.883	212.086	209.810	206.955	203.568	201.510	199.125	190.080	191.160	190.567
4	350.977	348.070	332.065	315.729	298.065	289.034	280.125	256.670	255.100	263.999
5	679.430	666.727	606.728	551.271	498.744	475.502	454.875	408.530	406.280	–

Table 3: Flexural-torsional buckling loads [N] for the axially compressed C-section beam

L/a	3D FEM [40]	$N=4$		$N=3$		$N=2$		TBM		EBBM	
		Ref. [40]	DSM	Ref. [40]	DSM	Ref. [40]	DSM	Ref. [40]	DSM	Ref. [40]	DSM
100	10.651	10.664	10.664	10.664	10.664	10.668	10.668	10.668	10.668	10.672	10.672
50	42.497	42.551	42.551	42.551	42.551	42.605	42.604	42.604	42.604	42.669	42.669
20	261.040	261.340	261.341	261.340	261.343	263.360	263.359	263.320	263.320	265.850	265.850
15	457.010	457.310	457.305	457.320	457.318	463.510	463.509	463.400	463.400	471.260	471.260

Table 4: Critical buckling loads [MPa] for various length-to-side ratio, L/a, of the SS square box beam

Model	Mode 1	Mode 2	Mode 3	Mode 4
Giunta et al. [40]				
3D FEM	10.651	42.443	95.008	167.780
$N=4$	10.664	42.551	95.339	168.500
$N=3$	10.664	42.551	95.339	168.500
$N=2$	10.668	42.604	95.607	169.340
TBM	10.668	42.603	95.602	169.330
EBBM	10.672	42.669	95.934	170.370
Present CUF-DSM				
$N=4$	10.664	42.551	95.339	168.507
$N=3$	10.664	42.551	95.339	168.507
$N=2$	10.668	42.604	95.607	169.340
TBM	10.668	42.603	95.603	169.327
EBBM	10.672	42.669	95.935	170.373

Table 5: First four buckling loads [MPa] of the SS square box beam for $L/a = 100$

L/h	Present CUF-DSM				Vo and Thai [7]		Aydogdu [18]
	$N=2$	$N=3$	$N=4$	$N=5$	FOBT	HOBT	
Material set I - [0°/90°/0°]							
5	4.992	4.668	4.667	4.666	4.752	4.709	4.726
10	6.937	6.751	6.750	6.749	6.805	6.778	–
20	7.677	7.618	7.618	7.617	7.630	7.620	7.666
50	7.917	7.904	7.904	7.903	7.897	7.896	–
Material set I - [0°/90°]							
5	1.856	1.831	1.820	1.816	1.883	1.910	1.919
10	2.140	2.130	2.126	2.125	2.148	2.156	–
20	2.226	2.223	2.222	2.222	2.226	2.228	2.241
50	2.252	2.252	2.252	2.252	2.249	2.249	–
Material set II - [0°/90°/0°]							
5	4.319	3.666	3.666	3.560	4.069	3.717	3.728
10	6.600	6.126	6.126	6.033	6.420	6.176	–
20	7.570	7.403	7.402	7.366	7.503	7.416	7.459
50	7.896	7.868	7.868	7.862	7.875	7.860	–
Material set II - [0°/90°]							
5	1.745	1.711	1.710	1.705	1.605	1.758	1.765
10	2.100	2.086	2.086	2.084	1.876	2.104	–
20	2.215	2.211	2.211	2.210	1.958	2.214	2.226
50	2.252	2.252	2.252	2.252	1.983	2.247	–

Table 6: Effect of length-to-height ratio, L/h , on the non-dimensional critical buckling loads ($P^*_{cr} = \frac{P_{cr}L^2}{E_2bh^3}$) of symmetric and anti-symmetric cross-ply SS laminated beams

BCs	Present CUF-DSM					Chattopadhyay and Radu [41]		
	EBBM	$N = 2$	$N = 3$	$N = 4$	$N = 5$	CLPT	FSDT	HOT
CF	16696	15752	15615	15607	15606	16344	15772	15364
CC	261957	163934	151256	151137	151132	261623	165644	152179

Table 7: Critical buckling loads [N] of the 8-layer cross-ply rectangular beam for different boundary conditions

Figures

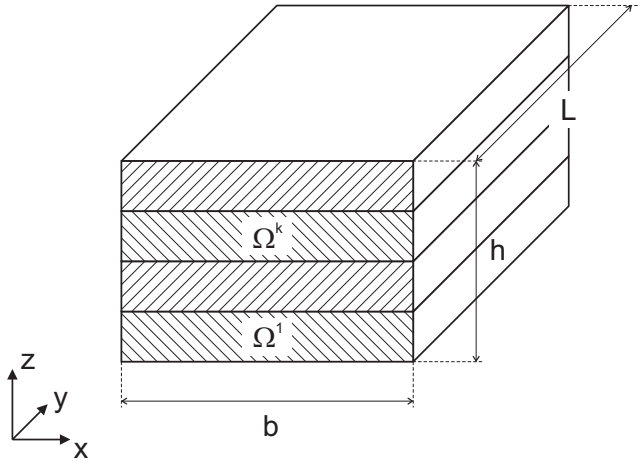

Figure 1: Geometry and reference system for a laminated composite beam

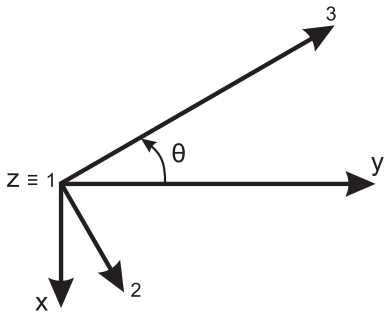

Figure 2: Fiber orientation angle

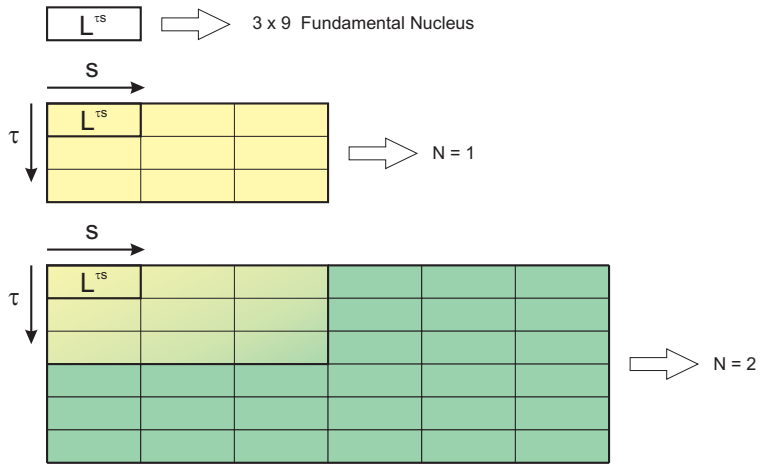

Figure 3: Expansion of the matrix $\mathbf{L}^{\tau s}$ for a given expansion order

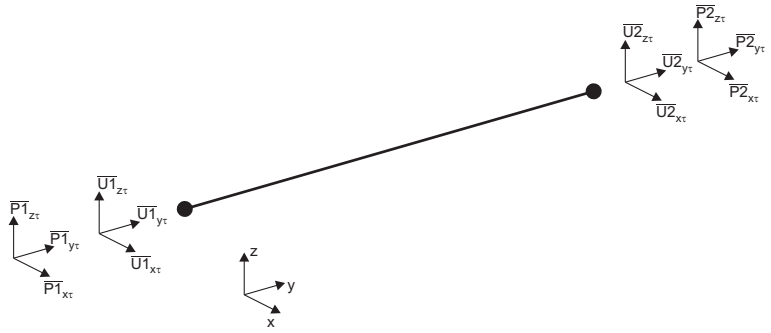

Figure 4: Boundary conditions of the beam element and sign conventions

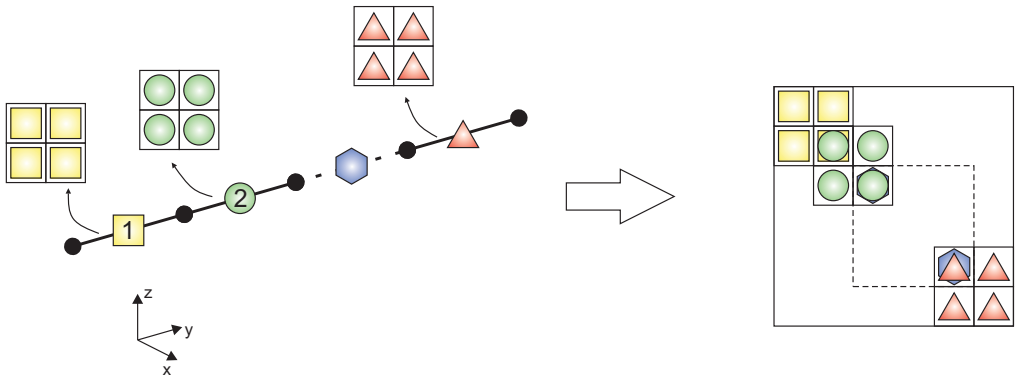

Figure 5: Assembly of dynamic stiffness matrices

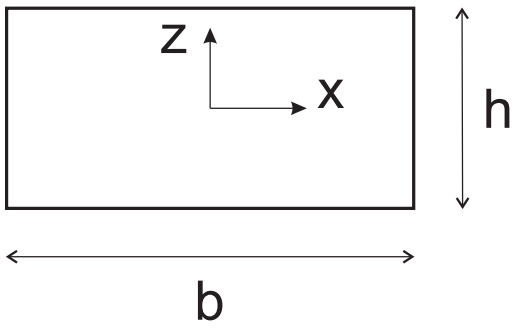

Figure 6: Rectangular cross-section

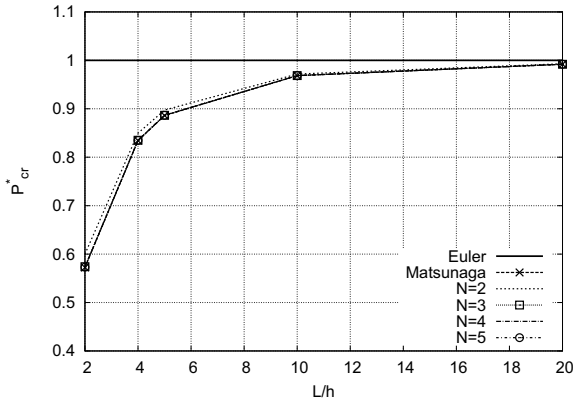

Figure 7: First non-dimensional critical buckling load ($P^*_{cr} = \frac{P_{cr} L^2}{\pi^2 EI}$) versus length-to-height ratio, L/h, for the rectangular metallic beam

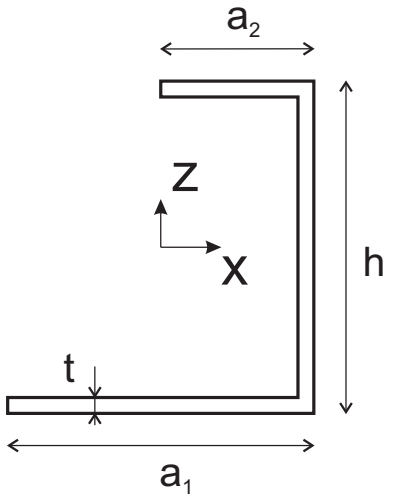

Figure 8: Cross-section of the C-shaped beam

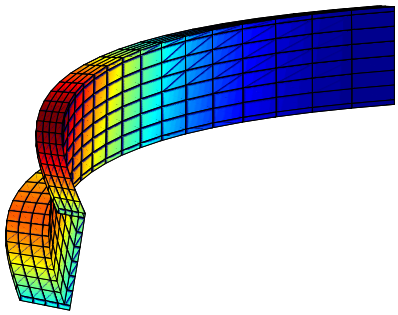

Figure 9: Second flexural-torsional buckling mode of the C-shaped section beam by the seventh-order ($N = 7$) CUF model.

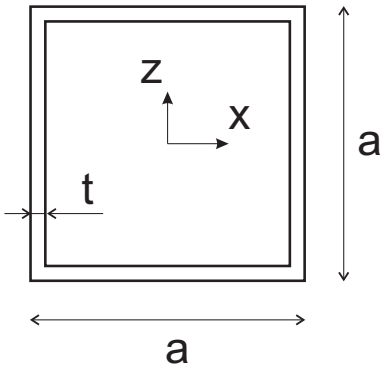

Figure 10: Cross-section of the box beam